

2015

Characterization of naïve immune cell subsets important in HIV/SIV pathogenesis as a baseline for RNASeq deconvolu

<https://hdl.handle.net/2144/16102>

"Downloaded from OpenBU. Boston University's institutional repository."

BOSTON UNIVERSITY
SCHOOL OF MEDICINE

Thesis

**CHARACTERIZATION OF NAÏVE IMMUNE CELL SUBSETS IMPORTANT IN
HIV/SIV PATHOGENESIS AS A BASELINE FOR RNASEQ DECONVOLUTION**

by

JESSICA NGUYEN

B.S., University of California Santa Barbara, 2011

Submitted in partial fulfillment of the
requirement for the degree of
Master of Science

2015

© 2015 by
JESSICA NGUYEN
All rights reserved

Approved by

First Reader

Jean L. Spencer, Ph.D.
Instructor of Biochemistry

Second Reader

James B. Whitney, Ph.D.
Assistant Professor of Medicine, Harvard Medical School

ACKNOWLEDGMENTS

I would like to acknowledge and thank the many people who helped make this past year both a fulfilling and a great learning experience. To Dr. James Whitney, I truly appreciate the opportunity to work in your lab group this past year. I learned so much and because of this experience, I see myself continuing to pursue research during my future medical career. To Dr. Christa Osuna, thank you very much for all of your help this past year. From teaching me how to aspirate without being afraid to making edits to this thesis, I could not have done it without you. I appreciate your patience when I first started and whenever I had questions. To Dr. So-Yon Lim and Sri Sanisetty, thank you for always offering to help and for making my experience here enjoyable. To Frances and Oscar, thank you for always making jokes and making long days in lab fun. I appreciate the constant lunchtime companionship and continual sarcasm in conversation. To Dr. Spencer, thank you for your help structuring and editing this thesis and for all of your help these past two years.

CHARACTERIZATION OF NAÏVE IMMUNE CELL SUBSETS IMPORTANT IN HIV/SIV PATHOGENESIS AS A BASELINE FOR RNASEQ DECONVOLUTION

JESSICA NGUYEN

ABSTRACT

The human immunodeficiency virus-1 (HIV-1) currently infects 35 million people globally. HIV preferentially infects CD4⁺ T cells, a critical component of the host immune system, causing their rapid depletion, which has a broad negative impact on host immunity. Chronic HIV infection also results in increased expression of inhibitory immune regulatory proteins, which is associated with impaired functionality of a wide range of immune cells. This clinical phenomenon, referred to as “immune exhaustion,” precludes the slow and eventual failure of host immunity against co-infecting pathogens and is the hallmark of AIDS-related disease.

In **Aim 1** of our studies, we used whole blood from Indian-origin rhesus monkeys to distinguish 12 discrete immune cell subsets utilizing antibody staining and flow cytometric cell sorting. The segregated “naïve” (uninfected) cell subsets will be characterized by RNASeq gene expression analysis, and will be used as the baseline population for a bioinformatics “deconvolution” method comparing the same cell subsets from simian immunodeficiency virus (SIV)-infected cell populations. We successfully developed an antibody panel that distinguishes activated and resting CD4⁺ T cells, activated and resting CD8⁺ T cells, activated and resting B cells, activated and resting NK cells, plasmacytoid dendritic cells, myeloid dendritic cells, and monocytes. We also developed a separate isolation protocol for neutrophils using different densities of

Percoll. Finally, we optimized cell sorting of CD4⁺ and CD8⁺ T cells in order to obtain sufficient amounts of high quality RNA for future RNASeq gene expression analysis.

As an adjunct to our above work, in **Aim 2** of our experiments we sought to quantify the expression of immune inhibitory proteins that are increased upon the various cell subsets during SIV infection. We set out to optimize an antibody panel targeting three proteins of interest, PD-L1, LAG-3, and TIM-3, for the study of whole blood from SIV-infected rhesus monkeys. This data will be used to compliment our RNASeq dataset developed in **Aim 1**. By utilizing a biotinylated antibody specific for PD-L1 along with fluorescently conjugated streptavidin, we were able to detect PD-L1-positive cells and allow for amplification of positive fluorescence. We also performed multiple evaluations of monoclonal antibodies specific to either LAG-3 or TIM-3 and determined the concentrations at which detection was best for LAG-3⁺ and TIM-3⁺ cells.

TABLE OF CONTENTS

TITLE.....	i
COPYRIGHT PAGE.....	ii
READER APPROVAL PAGE.....	iii
ACKNOWLEDGMENTS	iv
ABSTRACT.....	v
TABLE OF CONTENTS.....	vii
LIST OF TABLES.....	viii
LIST OF FIGURES	ix
LIST OF ABBREVIATIONS.....	x
INTRODUCTION	1
MATERIALS AND METHODS.....	16
RESULTS	20
DISCUSSION.....	37
LIST OF JOURNAL ABBREVIATIONS	46
REFERENCES	48
CURRICULUM VITAE.....	55

LIST OF TABLES

Table	Title	Page
1	Antibody Panels for Cytometric Immune Cell Subset Sorting	20
2	Total RNA Yield from Cytometric Cell Sorting	27

LIST OF FIGURES

Figure	Title	Page
1	Identification of immune cell subsets by flow cytometry	22
2	Identification and isolation of activated T cell subsets	23
3	Development of neutrophil isolation procedure	26
4	PD-L1 Staining of T cells stimulated with PMA/Ionomycin	30
5	PD-L1 titrations	31
6	LAG-3 titrations	33
7	TIM-3-A488 Staining	34
8	Detection of TIM-3 ⁺ T Cells with A488 and APC Conjugates	35

LIST OF ABBREVIATIONS

A488.....	AlexaFluor488
ACK.....	Ammonium-Chloride-Potassium
AIDS.....	Acquired Immunodeficiency Syndrome
APC.....	Allophycocyanin
APC γ	Antigen-Presenting Cell
ART.....	Antiretroviral Therapy
BV421.....	Brilliant Violet 421
CD4.....	Cluster of Differentiation 4
CD8.....	Cluster of Differentiation 8
CCR5.....	Cysteine-Cysteine Chemokine Receptor 5
ConA.....	Concanavalin A
CTLA-4.....	Cytotoxic T-lymphocyte Associated Protein 4
CXCR4.....	C-X-C Chemokine Receptor 4
DC.....	Dendritic Cells
EDTA.....	Ethylenediaminetetraacetic Acid
HIV.....	Human Immunodeficiency Virus
HTLV.....	Human T cell-lymphotropic Virus
IFN α	Interferon- α
IL-6.....	Interleukin-6
LAG-3.....	Lymphocyte Activation Gene-3
LTNP.....	Long Term Non-Progressor

mDC.....	Myeloid Dendritic Cell
MHC.....	Major Histocompatibility Complex
NHP.....	Non-Human Primate
NK.....	Natural Killer
PBMC.....	Peripheral Blood Mononuclear Cells
PBS.....	Phosphate-Buffered Saline
PD-1.....	Programmed Cell Death-1
pDC.....	Plasmacytoid Dendritic Cell
PE.....	Phycoerythrin
PE-Cy7.....	Phycoerythrin-Cyanine 7
PI3K.....	Phosphoinositide-3-Kinase
PMA.....	Phorbol 12-Myristate 13-Acetate
RBC.....	Red Blood Cells
RIN.....	RNA Integrity Number
RT.....	Room Temperature
SA.....	Streptavidin
SIV.....	Simian Immunodeficiency Virus
SLE.....	Systemic Lupus Erythematosus
T _H	T Helper Cell
Tat.....	Transactivator of Transcription
TCR.....	T Cell Receptor
TIM-3.....	T-cell Immunoglobulin Mucin-3

TNF α	Tumor Necrosis Factor- α
TLR.....	Toll-Like Receptor
Vif.....	Viral Infectivity Factor
WHO.....	World Health Organization

INTRODUCTION

HIV Etiology and Natural History-

At present, greater than 35 million people are infected globally with human immunodeficiency virus type-1 (HIV-1), and approximately 2 million people were newly infected in 2013¹. The vast proportion of this enormous disease burden is localized in underdeveloped regions, particularly Sub-Saharan Africa.

HIV-1 infection, left untreated, eventually leads to acquired immunodeficiency syndrome (AIDS). This disease state is characterized by a wide array of symptoms caused by immunologic exhaustion, resulting in multiple opportunistic infections that in many cases are fatal. The HIV-1 epidemic was first detected in the early 1980s as a result of an unusually high incidence of Kaposi's sarcoma cases and pneumocystis pneumonia, diseases not normally found in immunocompetent individuals, being reported in homosexual men in the United States². Similarly, in 1982, Gerstoft *et al.*³ described four cases in Copenhagen of homosexual men presenting in the clinic with symptoms of fever, severe weight loss, and lymphadenopathy. Each patient also demonstrated severe reductions in T helper cell subsets, poor cellular proliferation, decreased activity of natural killer (NK) cells, and impaired cytokine responses to normal antigens. At this time, the causative agent was unknown. Gerstoft had suggested a potentially infectious cause since each of the patients described had prior sexual contact with other homosexual men living in the United States where similar cases were becoming prevalent.

In 1983, Barré-Sinoussi and colleagues⁴ were able to isolate a virus from a homosexual male with a history similar to those patients described by Gerstoft *et al.*³.

This virus was similar, yet distinct, to a recently characterized retrovirus, human T-cell lymphotropic viruses (HTLV). Viral specific enzyme activity, termed “reverse transcriptase activity” was detected after donated T cells from a healthy individual were co-cultured with a sample taken from the lymph node of the patient described. A similar experiment was done with cell-free supernatants and again virus-specific reverse transcriptase activity was detectable. Interestingly, serum from the source patient did not react with antibodies specific to antigens from HTLV-1, and it was determined that the virus was distinct from known HTLV strains (types I and II). Thus, this new viral agent was subsequently named HTLV III and was considered to be the etiologic agent associated with the immunodeficiency syndrome. This nomenclature was later changed, and HTLV-III was re-classified to HIV and the disease was renamed AIDS.

HIV Structure and Genome-

HIV is a positive-sense, enveloped RNA virus containing “15 proteins and an RNA”⁵. The viral genome contains nine genes necessary for proper virion structure, replication, and infectivity: *gag*, *pol*, *env*, *tat*, *rev*, *vpr*, *vif*, *nef*, and *vpu*. The gene products of *gag*, *pol*, and *env* are important structural proteins and are translated as large protein precursors that are activated by cleavage with the viral protease. The major virus structural protein, termed the capsid (CA), and the nucleocapsid (NC) house the viral RNA genome as well as reverse transcriptase (RT), protease (PR), and integrase (INT). All of these components are critical for the early stages of the viral lifecycle following entry into the target host cluster of differentiation 4 (CD4)⁺ T cells. Many non-structural

gene products activate viral gene expression, such as the HIV transactivator of transcription (Tat) protein, while others are responsible for infectivity of newly produced virions, such as the viral infectivity factor (Vif) protein. Unlike human DNA polymerases, the viral reverse transcriptase has low replication fidelity, allowing many erroneous mutations to accumulate with each replication cycle. This high mutation rate leads to high HIV genetic diversity even within the same individual that is termed a viral swarm or quasispecies⁶. This mutation rate is a major feature of HIV-1 pathogenesis and underlies the ability of HIV to develop resistance to many antiretroviral treatments causing difficulty in the development of a prophylactic vaccine.

The viral envelope glycoprotein, gp120, which is anchored to the viral membrane by the gp41 viral protein, binds the CD4 receptor on a variety of host cells including CD4⁺ T cells, macrophages, and dendritic cells (DCs), and facilitates fusion entry into these cells⁷. Binding of gp120 to an additional co-receptor, predominantly either the cysteine-cysteine chemokine receptor 5 (CCR5) or C-X-C chemokine receptor 4 (CXCR4)^{8,9}, is also required for fusion and entry. The membrane envelope is acquired when a newly assembled virus buds from the host. Once released into the cytoplasm, the reverse transcriptase enzyme transcribes viral RNA into DNA. The viral integrase protein then facilitates the integration of HIV DNA into the host cell genome, thus establishing infection for the lifetime of the cell (and host). In many cells, the viral genome is quickly transcribed and translated to generate new progeny viruses. However, in a subset of cells, the viral DNA will remain transcriptionally silent, and the cell will become a reservoir for latent virus that has potential to be reactivated in the future¹⁰.

Two major types of HIV exist: HIV-1 and HIV-2. HIV-1 is more infectious and is therefore responsible for the majority of HIV infections worldwide¹¹. HIV-1 and HIV-2 share the same basic genome structure but sequence homology varies. Based on the sequences of two structural genes, *gag* and *env*, each HIV type is further classified into groups. For HIV-1, four major groups exist: M, N, O, and P. Group M (major) is responsible for most HIV-1 infections and can be further divided into nine subtypes¹². HIV-2 is divided into five groups.

HIV-1 Infection-

A variety of immune cells are susceptible to HIV infection. Macrophages and DCs can be infected; however, CD4⁺ T cells are the predominant targets¹³ and are rapidly infected and depleted during acute HIV-1 infection. After several weeks, CD4⁺ T cell numbers are partially restored, although they exhibit dramatically impaired functionality, including decreased proliferation and cytokine production, a condition termed “T cell exhaustion”¹⁴.

In HIV-1 infected patients, infectious virus can be isolated from multiple sources, including blood, semen, vaginal secretions, and cerebrospinal fluid. Transmission can occur through exchange of infected body fluids during sexual intercourse, from use of contaminated needles, from mother to child, and from blood transfusions or organ transplantation. While sexual intercourse is a significantly lower-risk transmission route compared to others, it accounts for the majority of HIV cases worldwide. HIV-1

infection can be increased by additional factors; for example, presentation of a genital ulcer disease can enhance transmission rates.

The World Health Organization (WHO) defines four major stages of HIV-1 disease. Patients in stage 1 are highly infectious, have relatively normal CD4 T cell counts, and have no detectable HIV-specific antibodies. Patients in stage 2 have rapidly increasing viral loads with accompanying decreases in CD4 T cell counts, and appearance of HIV-specific antibodies. Patients in stage 3 become increasingly immunocompromised, have CD4 T cell counts from 200-500 cells per microliter, and exhibit symptoms such as chronic diarrhea, severe weight loss, and fever. Patients in stage 4 have CD4 T cell counts below 200 cells per microliter, are at high risk for opportunistic infections, and are highly infectious.

Without intervention, CD4⁺ T cell numbers as well as immune function continually decline during the chronic stages of infection, resulting in AIDS within a several years of infection. Patients in advanced stages develop “AIDS-defining malignancies” which include Kaposi’s sarcoma, non-Hodgkin’s lymphoma, and cervical cancer¹⁵. The rate of disease progression varies dramatically within affected individuals. HIV-1 infected individuals can remain asymptomatic for many years. During this latent period, individuals may present with vague symptoms such as fever or swollen lymph nodes that are typically attributed to other non-specific viral infections. Three patterns of disease progression exist: typical, rapid, and long-term non-progressors. Typical progressors comprise 50%-70% of those affected and disease progresses over 8-10 years. Rapid progressors comprise 5%-10% of those affected and disease progresses over 2-3

years. Long-term non-progressors (LTNPs) comprise 5% of those affected. They maintain normal CD4⁺ T cell counts, have viral loads below the level of detection of standard viral load assays, and are able to live without disease progression for greater than 10 years. LTNPs have been extensively investigated in order to understand the genetic, environmental, and immune components that contribute to superior viral control with the hope of advancing HIV prevention and therapy.

With the advent of antiretroviral therapy (ART), patients have been able to live much longer and with improved quality of life. However, despite the vast benefits of ARV therapy, patients remain at risk for development of end-organ diseases and cumulative ART drug toxicity¹⁶. In addition, because ART only targets cells with actively replicating virus and does not impact latently infected cells, virus cannot be completely eradicated from infected individuals. Therefore, alternative therapies to eradicate or “cure” patients need to be explored. Some of these therapies aim to target these latently infected cells with the goal of complete virus eradication, termed “sterilizing cure”. However, at present this goal is unlikely to be clinically achievable. Other therapies may be more practical, such as purging latent virus from hiding, boosting the immune system so an infected individual can control viral replication in the absence of ART, or a combination of both. These types of therapies have been termed “functional cure”.

HIV and the Immune System

HIV preferentially targets activated CD4⁺ T cells¹⁷. The chromatin in these cells, as opposed to resting CD4⁺ T cells, is in a state that permits viral DNA integration. As a

result, these cells can support the entire viral lifecycle. While most infected cells die quickly, a small subset reverts to a resting state of either central or transitional memory¹⁸ to establish the latent reservoir¹⁹. These memory subsets are ideal reservoirs because they are long-lived and in a resting state.

Even in the presence of therapy, HIV causes chronic hyper-immune activation. Levels of interleukin-6 (IL-6), a pro-inflammatory cytokine, were 40%-60% higher in HIV⁺ individuals on suppressive drug therapy compared with well-matched healthy controls¹⁹. Moreover, the gut mucosa is densely populated with susceptible cells expressing the CD4 receptor and the CCR5 co-receptor. Infection of this dense cell population is thought to be the cause of irreversible damage to the mucosal barrier leading to constant antigen exposure and local immune activation^{16,18,20}. Hyperimmune activation is characterized by highly activated monocytes and macrophages but these cells exhibit decreased phagocytosis, defective cytokine production and antibody-dependent cell-mediated cytotoxicity of NK cells, and a dysfunctional phenotype of T cells²⁰. Wilson *et al.*²¹ examined immune hyper-activation in the context of lymphocytic choriomeningitis infection in mice. One strain was capable of rapid clearance, while the other strain established a chronic infection. Mice with chronic infection showed sustained elevation of type 1 interferon that was correlated with more rapid disease progression. Antigen-presenting cells (APC γ) of chronically infected mice also displayed high expression of negative immune regulators and antibody blockade of these negative regulators led to improved viral control. Despite the advances of long-term suppressive

ART, individuals still remain at high risk for development of cardiovascular disease, neurodegenerative disease, osteoporosis, liver damage, kidney failure, and cancer¹⁶.

Extensive research has gone into the immune responses that are most important for viral control. Toll-like receptors (TLRs) have been described as the first “immune sensors” activated by infection with HIV-1²². TLR7 and TLR8 are able to recognize single-stranded RNA. Recognition of single-stranded RNA by TLR7 on DCs has been shown to cause increased secretion of interferon- α (IFN α) and tumor necrosis factor α (TNF α)²³. NK cells are continually surveying the body for foreign invaders and are important in the control of virus replication²⁴. In murine cytomegalovirus, NK cells expressing a specific activating receptor, Ly49H, were able to detect a viral protein product and rapidly expand in response²⁵. Alter *et al.*²⁶ also investigated this phenomenon in HIV-1 infection in 2009. Though it was known that NK cells expanded rapidly during acute HIV-1 infection, it was unknown whether this was non-specific or specific to NK cells expressing the human homolog of Ly49H. NK cells expressing this human homolog were found to be specifically expanded during acute HIV infection²⁶.

Because CD4⁺ T cells are preferential viral targets and essential for many important immune functions, CD4⁺ T cell counts during infection correlate with disease progression and modulations in viral load. Clinically, CD4⁺ T cell counts are also the basis for initiation of ART²⁷. CD4⁺ T cell counts are normal in LTNPs and their peripheral blood mononuclear cells (PBMCs) display an antiapoptotic and pro-T cell survival expression profile²⁸. LTNPs also exhibited fewer numbers of memory and naïve

CD4⁺ T cells expressing one of the required co-receptors, CCR5, than those with normal HIV-disease progression²⁹.

Simian Immunodeficiency Virus and Non-Human Primate Models of HIV

Natural primate hosts of simian immunodeficiency virus (SIV), such as sooty mangabeys and African green monkeys, exhibit chronic infection with high levels of viremia but remain asymptomatic. Infection in a non-natural host such as Asian origin macaques produces a disease profile similar to HIV-1 infection in humans³⁰. Comparison of disease progression of SIV in natural and non-natural hosts has been useful to studying HIV pathogenesis. For example, in nonpathogenic infection of natural SIV hosts, low levels of infection were seen in CD4⁺ central memory T cells, which strongly suggested this cell subset as a key factor in the pathogenesis of HIV infection^{31,32}. Use of non-human primate (NHP) models has also been essential in understanding HIV susceptibility and pathogenesis, and in developing prophylactic and therapeutic interventions. The model allows for control of multiple parameters that are otherwise impossible to control for in humans, such as time of infection, dose, and route of exposure. It also permits extensive sampling of cell and tissue samples from noninfected and infected animals. For example, it has resulted in the in-depth understanding of the role of CD4⁺ T cells and the destruction of secondary lymphoid tissues such as the gut mucosa³³. The rapid depletion of CD4⁺ T cells is associated with enhanced viral replication, infection of a large population of macrophages, and faster disease progression³⁴. Destruction of the gut mucosa results in the movement of microbial products into systemic circulation,³⁵ and

contributes to the chronic inflammatory state already present, and parallels the same condition in HIV-infected patients.

HIV Vaccine and Therapeutic Research-

The rhesus monkey/SIV model also permits testing of experimental interventions. Many candidate vaccines against HIV are being developed and evaluated using this model system. In addition, vaccine approaches, such as live attenuated vaccines, have been explored with this model. For example, rhesus monkeys, after being vaccinated with a modified non-pathogenic SIV strain (SIVmac239delta-Nef), and challenged with a subsequent pathogenic SIV strain showed unique protective cluster of differentiation 8 (CD8)⁺ T cell gene expression profiles. Expression of genes involved in T cell activation, differentiation, signaling, and adhesion was enhanced relative to nonvaccinated controls³⁶. Two of the six animals inoculated were resistant to infection with the pathogenic strain and the remaining four animals showed substantially improved viral control compared with nonvaccinated controls. However, long-term follow-up of these animals indicated signs of virus mutation back to full pathogenicity--an unexpected setback to the field. Nevertheless, the testing of this modality in monkeys revealed a future danger that was circumvented had clinical trials in humans been considered.

Many other candidate vaccines, such as adeno-associated vaccines, T-cell based vaccines, and recombinant herpes vaccines, are being investigated but few have been evaluated in human clinical trials. With the recent interest in attaining stabilizing and

functional cures of HIV-infected individuals, the NHP model continues to be vital to our understanding and treatment of HIV infection.

Immune anergy, exhaustion, and replicative senescence all describe impaired T cell effector function, a situation exacerbated in chronic HIV infection. Constant exposure to foreign antigen leads to expansion of effectors with impaired function, increased suppressor T cell numbers, and lack of generation of memory cell subsets. Impaired T cell function is predominantly attributed to the up-regulation of negative co-stimulatory molecules including programmed cell death 1 (PD-1) and its ligands, PD-L1 and PD-L2, lymphocyte activation gene-3 (LAG-3), and T-cell immunoglobulin mucin-3 (TIM-3). Expression of these molecules varies across immune cell types and is either constitutive or inducible after T cell activation. Each has distinct mechanisms of inhibition and effects of binding can be synergistic. In healthy individuals, these molecules work to prevent tissue damage caused by strong immune responses but in chronically ill patients, such as those with HIV, these molecules help to perpetuate infection by dampening immune responses. The involvement of these molecules in HIV pathogenesis has been extensively investigated and there is substantial interest in understanding how modulating their expression or function can reinvigorate immune responses. Because there has been success with antibody blockade of these molecules in the treatment of hematologic and solid cancers in which a similar hyper-activated immune system also exists³⁷, a similar treatment may be efficacious in treating HIV.

Aims of Present Study

Aim 1. Isolation of Cells and RNA for Gene Expression Deconvolution

Essentially all immune cell subsets are modulated during HIV infection. Therefore, it is important to understand not only the basic biology of these cells, but also how they may be modulated or targeted for HIV prevention or therapy. There are numerous immune cell subsets that can be broadly classified into erythrocytes, platelets, T cells, B cells, NK cells, dendritic cells, monocytes, macrophages, mast cells, neutrophils, eosinophils, and basophils. Each of these cell subsets can be further separated into more detailed cell subsets. For example, T cells can be broadly categorized as CD4⁺ T cells or CD8⁺ T cells, and each of these groups can be further categorized based on its differentiation state, which is broadly classified as naïve (has not seen antigen), effector, or memory. Each of these differentiated subsets can be further broken down based on permutations of many other parameters, such as activation status, cytokine production profile, and transcriptional profile. This latter measure is the most sensitive characteristic for distinguishing discrete cell subsets³⁸. Usually, each of these cell subsets is studied in isolation or with limited simultaneous consideration of other subsets. Nevertheless, to fully understand the dynamic interplay of the virus on the immune system, more complex approaches are required.

Development of whole genome expression profiling has substantially expanded our ability to perform highly complex analyses. With the right bioinformatics tools, gene expression analysis can identify not only expression changes in a cell subset that are associated with different conditions, such as healthy versus diseased individuals, but also

changes that occur simultaneously in multiple cell subsets within an individual. Historically, in order to perform analyses at the cell subset level, individual cell subsets had to be isolated, and the gene expression profile had to be measured for each subset. These procedures are technically challenging, time consuming, and also very expensive.

Recently, a bioinformatics method termed “expression deconvolution” has been developed, which allows for the teasing apart of gene expression contributions from discrete cell subsets within datasets generated from heterogeneous samples such as whole blood. This method is based on the ability to estimate the proportion of the sample to which each cell subset contributes. From this information, one can then attribute the changes in gene expression in the sample to a specific cell subset. The validity and utility of this analysis has been applied to multiple settings. For example, this technique was used with known microarray data and a basis matrix in order to elucidate the different cell types in blood samples taken from a clinical study. The investigators were able to accurately predict the mixing proportions of cell types in the samples, which allowed for more accurate analysis of the expression data³⁹.

In Aim 1 of our research, we are interested in applying expression deconvolution analysis in order to enhance gene expression analyses of whole blood samples from SIV-infected rhesus monkeys involved in experimental SIV therapies. However, deconvolution analysis requires an algorithm based on the known expression profiles of the individual cell subsets that comprise the sample of interest. This requires isolation and gene expression profiling of each individual subset. While such an algorithm has been developed for multiple types of human samples, one does not currently exist for rhesus

monkeys. We will contribute to establishing this algorithm for rhesus monkeys by developing methods to target immune cell subsets from peripheral blood for identification and cells sorting for the isolation of associated RNA.

Aim 2. Evaluation of Immune Checkpoint Antibody Panels

HIV causes not only rapid depletion of immune cells but also impaired functionality of remaining cells. Virus-specific T cells exhibit functional senescence and have impaired cytokine production¹⁴. T cell responses require two signals: (1) stimulation by antigen bound to the major histocompatibility complex (MHC) of APCs at the T cell receptor (TCR) and (2) co-stimulation by either positive or negative regulatory molecules. Infection leads to sustained elevation of pro-inflammatory cytokines²¹ that contribute to a state of immune hyperactivation despite control of viremia.

Immune hyperactivation leads to increased expression of inhibitory molecules on immune cells in an attempt to limit immune-mediated tissue damage. Binding of these inhibitory molecules, also called immune checkpoint molecules, promotes the downregulation of T cells by means of distinct mechanisms. For example, PD-1 binding to its cognate ligands, PD-L1 or PD-L2, directly antagonizes TCR and CD28 activation of phosphoinositide-3 kinase (PI3K), which results in reduced T cell glucose metabolism¹⁴. Considerable research has gone into developing treatments that will eradicate virus from the body by targeting these checkpoint molecules. Inhibitory molecules such as LAG-3, TIM-3, and PD-1, as well as its ligands, PD-L1 and PD-L2,

are being investigated to more clearly identify their roles in T cell dysfunction and T cell exhaustion.

In Aim 2 of our research, we will explore the expression of selected immune inhibitory proteins in both SIV-infected and noninfected animals. In particular, because of their central role in defective immune responses, we will examine three molecules, PD-L1, LAG-3, and TIM-3. Using whole blood of SIV-infected and noninfected rhesus monkeys, we will develop a strategy utilizing antibody staining and flow cytometry to quantify expression of these checkpoint molecules.

MATERIALS AND METHODS

Deconvolution

Animals

Indian-origin rhesus monkeys (*Macaca mulatta*) were housed at Bioqual Inc. (Rockville, MD) in accordance with the guidelines outlined in the National Institutes of Health *Guide for the Care and Use of Laboratory Animals* and with the approval of the Institutional Animal Care and Use Committee of Harvard Medical School and the National Institutes of Health.

Sample Processing for Peripheral Blood Mononuclear Cells (PBMCs)

Ethylenediaminetetraacetic acid (EDTA)-preserved blood whole blood was typically first centrifuged at 2500rpm for 15min at room temperature (RT) and the buffy coat layer of leukocytes was collected. These cells (or whole blood directly, if no buffy coat was isolated first) were layered onto Ficoll (1.077 g/mL) (GE Healthcare, Pittsburgh, PA) to isolate PBMC by density gradient centrifugation. PBMCs were collected and rinsed with a wash buffer of 1X phosphate-buffered saline (PBS) (Gibco; Life Technologies, Carlsbad, CA) supplemented with 2% heat-inactivated fetal bovine serum (FBS) (HyClone, GE Healthcare, Pittsburgh, PA). When necessary, red blood cells were removed by lysis with ammonium-chloride potassium (ACK) buffer (150mM ammonium chloride, 10mM potassium bicarbonate, and 30mM EDTA in water) for 3-5 minutes, followed by rinsing with wash buffer. PBMCs either were used immediately or cryopreserved in 10% dimethylsulfoxide (DMSO) in FBS and thawed upon use.

Cryopreserved PBMC were thawed for 1min in 37°C water bath and washed with pre-warmed RPMI 1640 medium (Cellgro, Corning, NY) with 10% FBS.

Antibody Staining for Flow Cytometry

If PBMC were cryopreserved, PBMCs were re-suspended in 1XPBS and stained with Amine Live/Dead viability dye (Invitrogen, Cambridge, MA) for 20min at RT in the dark and then washed with 1XPBS. Fresh or cryopreserved PBMCs were then re-suspended in wash buffer and stained with antibody cocktails in the dark at RT for 15min. Cells were washed once, re-suspended in a solution of 2% paraformaldehyde (Polysciences, Inc., Warrington, PA) in 1XPBS (fix buffer), and analyzed by flow cytometry using a BD LSRII Analyzer (BD Biosciences, San Jose, CA). Data were analyzed on FlowJo software (FlowJo, LLC, Ashland, OR).

Flow Cytometric Cell Sorting

Antibody-stained cells were re-suspended in 1XPBS and maintained on ice. Cells were sorted using a BD FACS Aria cell sorter (BD Biosciences, San Jose, CA). Sorted cells were either collected either into RNA Protect (QIAGEN, Valencia, CA) at RT or into TRIzol LS (Life Technologies, Carlsbad, CA) at RT. Cells sorted into RNA protect were centrifuged at 1,000 x g for 10min, supernatant aspirated, and then resuspended in standard TRIzol (Life Technologies, Carlsbad, CA) and stored at -80°C. Cells sorted into TRIzol LS were directly stored at -80°C.

Neutrophil Isolation

Stock Percoll (1.13 g/mL) (GE Healthcare, Pittsburgh, PA) was made isotonic by combining 9 parts stock Percoll with 1 part 10X PBS. The density of the isotonic Percoll, as well as the calculations for volumes needed to make less dense Percoll solution from the isotonic Percoll, were determined using the following equation:

$$V_x = V_0 \frac{(\rho_0 - \rho_i)}{(\rho_i - \rho_m)}$$

V_0 is the volume of starting Percoll. ρ_0 is the density of starting Percoll. ρ_i is the density of solution that the Percoll will be diluted in. ρ_m is the target density of the diluted Percoll solution. V_x is the volume of diluting solution required to reach the target density given the volume of starting Percoll (V_0). The densities of diluting medias (either 1XPBS or RPMI1640) were assumed to be the same, at 1.006 g/ml)

Heavy Percoll was layered beneath 1.077 g/mL Percoll. Buffy coat sample was layered on top of 1.077 g/mL Percoll. The sample was centrifuged at 3000rpm for 20-30min at RT. Cells at the interface between the light and heavy Percoll's, as well as cells above the 1.077 g/mL layer and cells within both Percoll layers, were collected and washed with wash buffer. Cells were either directly resuspended in fix buffer or first stained with indicated antibodies, washed, and then resuspended in fix buffer.

RNA Isolation and Quantification

The cells in frozen in TRIzol were thawed and spun down at 12,000 x g for 15min at 4°C. The aqueous top layer was removed and an equal volume of 100% ethanol was

added. The sample was then transferred to an RNeasy mini spin column (QIAGEN, Valencia, CA). The sample was centrifuged for 15 s at 8000 x g and the supernatant was discarded. The sample was then processed according to the manufacturer's instructions (Qiagen RNeasy Kit, Valencia, CA). Isolated RNA was analyzed on an Agilent 2100 bio-analyzer using either a Pico or Nanochip (Agilent Technologies, Santa Clara, CA).

Flow Cytometry "Exhaustion Panel" Optimization

Antibody staining for flow cytometry

If PBMC were cryopreserved, PBMCs were resuspended in 1XPBS and stained with Amine Live/Dead viability dye for 20min at RT in the dark and then washed with 1XPBS. Fresh or cryopreserved PBMCs were then resuspended in ice-cold wash buffer. For staining with biotinylated antibodies, cells were incubated on ice with the antibody for 1hr. Cells were then wash twice with ice-cold wash buffer. Cells were resuspended in ice-cold wash buffer. Fluorescently labeled antibodies were then added. If already stained with biotinulated antibody, cells were also simultaneously stained with fluorescently labeled streptavidin (SA). Cells were incubated on ice for 30min in the dark. Cells were then washed twice in wash buffer, resuspended in fix buffer, and collected on the BD LSRII Analyzer. Data were analyzed on FlowJo software (Tree star).

RESULTS

Aim 1. Isolation of Cells and RNA for Gene Expression Deconvolution

Flow Cytometric Antibody Panel Development

Major immune cell subsets in the peripheral blood were selected to be sorted for RNA expression analysis: neutrophils, plasmacytoid dendritic cells (pDCs), myeloid dendritic cells (mDCs), monocytes, B cells, CD4⁺ T cells, CD8⁺ T cells, and NK cells. Cell surface protein expression patterns were used to define each of these target subsets. B cells, CD4⁺ T cells, CD8⁺ T cells, and NK cells were separated further into resting and activated subsets (Table 1).

Panel Name	Antigens Detected	Target Populations	Cell	Cell Population Definition
T Cells	CD3, CD4, CD8, CD38, HLA-DR	CD4 ⁺ Resting		CD3 ⁺ CD4 ⁺ CD8 ⁻ CD38 ⁻ HLA-DR ⁻
		CD4 ⁺ Activated		CD3 ⁺ CD4 ⁺ CD8 ⁻ CD38 ⁺ HLA-DR ⁺
		CD8 ⁺ Resting		CD3 ⁺ CD4 ⁻ CD8 ⁺ CD38 ⁻ HLA-DR ⁺
		CD8 ⁺ Activated		CD3 ⁺ CD4 ⁻ CD8 ⁺ CD38 ⁺ HLA-DR ⁺
NK/B Cells	CD3, CD8, CD14, CD20, CD69, NKG2A	B cell Resting		CD3 ⁻ CD14 ⁻ CD20 ⁺ CD69 ⁻ NKG2A ⁻
		B Cell Activated		CD3 ⁻ CD14 ⁻ CD20 ⁺ CD69 ⁺ NKG2A ⁻
		NK Resting		CD3 ⁻ CD8 ⁺ CD14 ⁻ CD20 ⁻ CD69 ⁻ NKG2A ⁺
		NK Activated		CD3 ⁻ CD8 ⁺ CD14 ⁻ CD20 ⁻ CD69 ⁺ NKG2A ⁺
DC/Monocytes	NKG2A, CD3, CD20, CD14, HLA-DR, CD123, CD11c	Monocytes		NKG2A ⁻ CD3 ⁻ CD20 ⁻ CD14 ⁺
		DC-plasmacytoid		NKG2A ⁻ CD3 ⁻ CD20 ⁻ CD14 ⁻ HLA-DR ⁺ CD123 ⁺ CD11c ⁻
		DC-myeloid		NKG2A ⁻ CD3 ⁻ CD20 ⁻ CD14 ⁻ HLA-DR ⁺ CD123 ⁻ CD11c ⁺

Table 1 Antibody Panels for Immune Cell Subset Sorting

Activated T cells were defined initially by co-expression of HLA-DR and CD38^{40,41} while activated B cells and NK cells were defined by expression of CD69. Based on our definition of each cell subset, three panels of fluorochrome-labeled antibodies were selected to identify and sort each subset by flow cytometry (**Table 1**). Neutrophils were to be identified by light scattering properties alone. Each of the three antibody panels were evaluated for the presence of unfavorable interactions between fluorochromes and the ability to clearly identify the cell subsets of interest.

PBMCs were isolated from whole blood samples from SIV-naïve rhesus monkeys using Ficoll density gradient centrifugation and cell samples were stained with each of the test panels. Representative staining and gating for each panel is shown in **Figure 1**. For each panel, cell doublets were excluded and live cells were selected from within the single cell population. Among the live cells, a large gate was created that included both lymphocytes and monocytes (**Figure 1A**). From within this gate, either T cells, B cells and NK cells, or monocytes and DCs were analyzed, depending on the panel. For the T cell panel, expression of CD3 was used to identify T cells, which were subsequently separated into CD4⁺ and CD8⁺ T cells (**Figure 1B**). For the B cell and NK cell panel, CD14⁺ monocytes were first excluded. B cells were identified by expression of CD20 and lack of expression of NKG2A. NK cells were identified by lack of expression of CD20 and co-expression of CD8 and NKG2A (**Figure 1C**). In the monocyte and DC panel, T cells, B cells, and NK cells were excluded by selecting CD3⁻CD20⁻NKG2A⁻ cells. Monocytes were identified based on expression of CD14. DCs were identified based on the lack of expression of CD14 and the expression of HLA-DR. The pDCs and mDCs

were further identified based on expression of CD123 and CD11c respectively (**Figure 1D**).

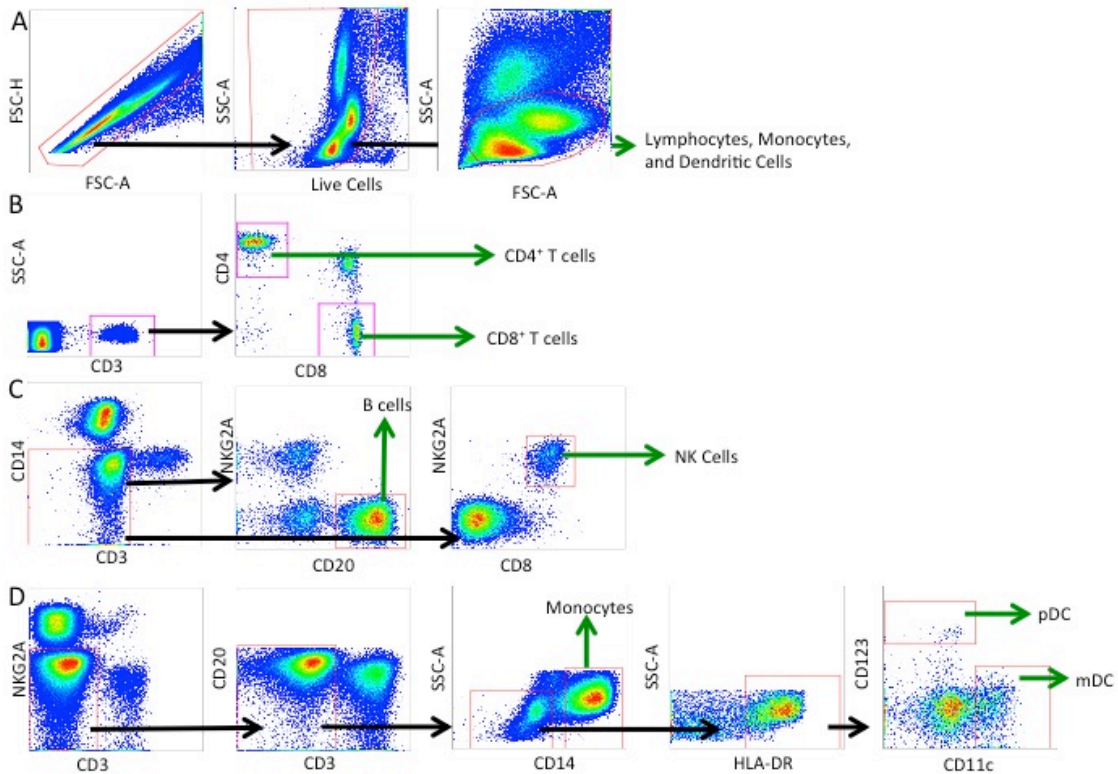


Figure 1 Identification of immune cell subsets by flow cytometry

Flow plots show representative staining and identification of immune cell subsets from rhesus PBMC samples. (A) Initial gating strategy used for all antibody panels to exclude cell doublets and dead cells, and select lymphocytes and monocytes for further analysis. (B) T cell panel (C) NK/B cell panel (D) DC/monocyte panel. Black arrows indicate the selection of a cell subset used in subsequent gating. Green arrows indicate the final subset selected.

This analysis indicated that there were not any unfavorable interactions between fluorochromes. In addition, all target populations could be clearly identified. However, the frequency of CD38⁺HLA-DR⁺ T cells was extremely low and would be insufficient

for sorting (**Figure 2A**). To address the low frequency of these CD38⁺HLA-DR⁺ T cells, the combination of HLA-DR and CD38 as the definition of an activated T cell was replaced with CD69 as an activation marker ⁴². To confirm that this revised panel was appropriate, cryopreserved PBMC from two monkeys were stained with the updated T cell antibody panel and analyzed by flow cytometry.

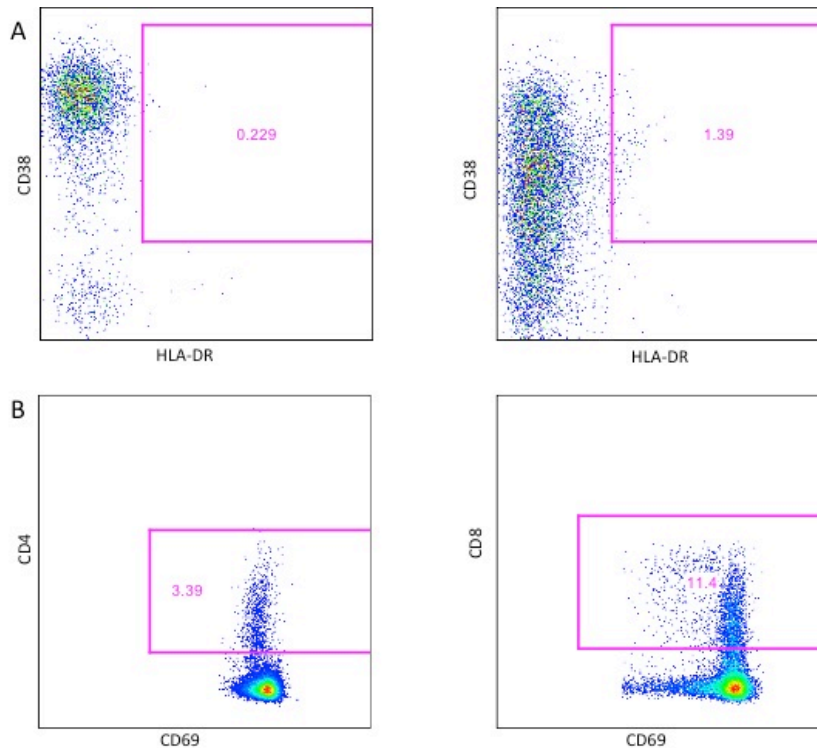


Figure 2 Cytometric identification of activated T cell subsets

Flow plots show rhesus PBMCs that were stained with antibody panels containing either HLA-DR and CD38 or CD69 to identify activated T cells. (A) T cell panel containing HLA-DR and CD38. (B) T cell panel containing CD69. Right: CD4⁺ T cells. Left: CD8⁺ T cells.

The frequency of CD69⁺ T cells was substantially higher than CD38⁺HLA-DR⁺ T cells in the previous samples (**Figure 2B**) and was considered appropriate for sorting. Moreover, there were no apparent adverse interactions between fluorochromes in this revised panel.

From our antibody panel evaluations, we determined that neutrophils could not reliably be identified by light scattering properties alone (data not shown). To address this issue, we developed a separate neutrophil isolation procedure. Also, because red blood cell (RBC) contamination in our first panel evaluation exacerbated the difficulty in neutrophil identification, we added a density centrifugation step prior to all cell isolation protocols that allowed for separation of RBCs from total white blood cells (buffy coat).

To isolate neutrophils, we first evaluated a commercially available separation solution comprised of diatrizoate and Dextran 500 (Cedarlane Laboratories, Burlington, Ontario, Canada), which had been previously used to isolate neutrophils from human blood samples⁴³. Because this solution was too dense, no cells from rhesus peripheral blood passed through the solution after centrifugation (data not shown). We subsequently evaluated a commercially available Ficoll solution with density of 1.084 g/mL. We layered this heavier Ficoll beneath the standard Ficoll solution with density of 1.077g/mL. As expected, six layers were visible after centrifugation for 20 minutes. The PBMC layer, 1.077 g/mL Ficoll layer, presumed neutrophil layer, and 1.084 g/mL Ficoll layer were each harvested and analyzed by flow cytometry. The top layer of media and the RBC pellet were discarded. Samples were evaluated for percent neutrophil enrichment by determining percentage of neutrophils. Representative data for this

analysis are shown in **Figure 3A**. The presumed neutrophil layer was enriched in neutrophils, as determined by their forward-scattered (FSC) light and side-scattered (SSC) light properties. However, there was also a substantial amount of neutrophils that had passed into the 1.084 g/mL Ficoll layer.

We next evaluated two densities of Percoll, 1.0875 g/mL and 1.09 g/mL, layered under Percoll of density 1.077 g/mL. As expected, these samples also formed six distinct layers after a 20-minute centrifugation. Again, the PBMC layer, 1.077 g/mL Percoll layer, presumed neutrophil layer, and each of the heavier Percoll layers were each harvested. For enhanced identification of neutrophils, samples were stained with fluorochrome-labeled antibodies specific to CD14 and CD11b and analyzed by flow cytometry. Neutrophils are CD11b⁺ and CD14^{dim}. Representative data for this analysis are shown in **Figure 3B,C**.

In our first round of isolation using Percoll, we obtained greater than 95% neutrophils in the neutrophil layer. However, there were a substantial number of neutrophils that remained in the 1.077 g/mL Percoll layer. A considerable number of neutrophils were also found in the heavier Percoll layers, although there were relatively fewer neutrophils in the 1.09 g/mL layer than in the 1.0875 g/mL layer. We repeated these isolation procedures and increased our centrifugation time to 30 minutes. By doing this, we were able to pull down the neutrophils from the 1.077 g/mL Percoll layer into the neutrophil layer and at the same time retain substantial enrichment of neutrophils in the presumed neutrophil layer. Greater numbers of neutrophils passed into the 1.0875 g/mL

Percoll layer compared with the 1.09 g/mL. Based on these results, we chose the 1.09 g/mL Percoll for future neutrophil isolations.

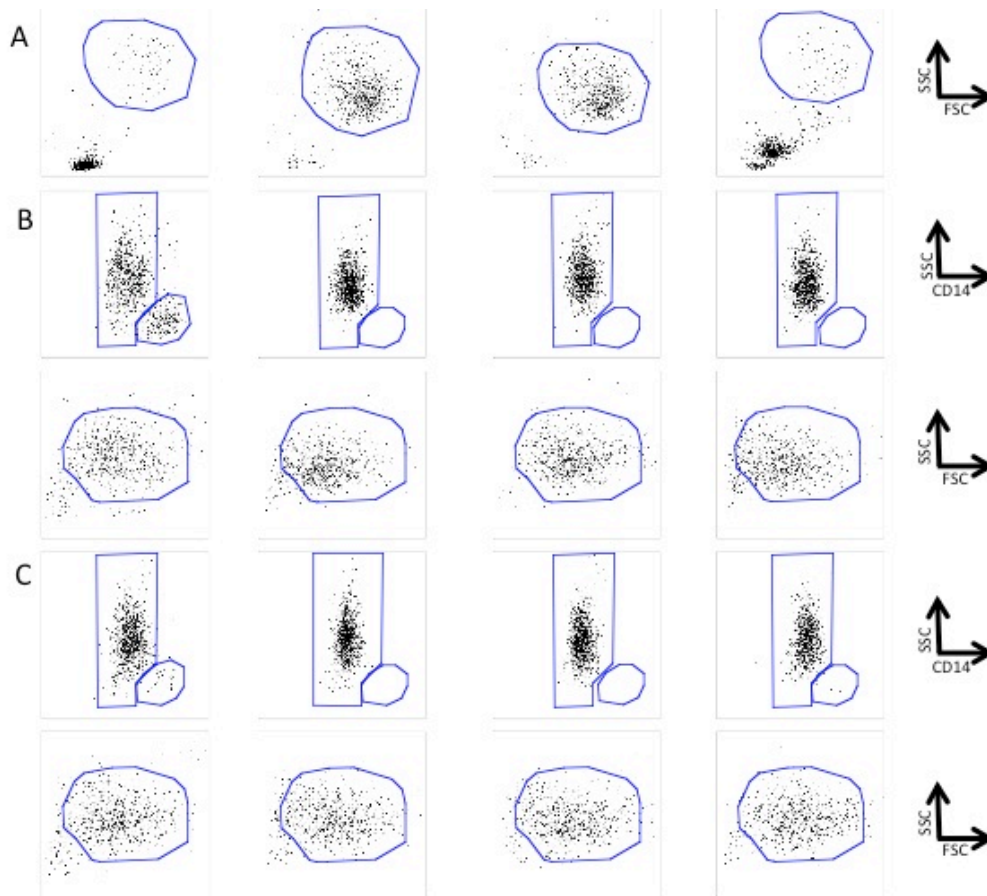


Figure 3 Development of neutrophil isolation procedure

(A) Neutrophil isolation using 1.084 g/mL Ficoll. 2,000 cells are displayed in each plot. Neutrophils were gated based on light scattering properties. (B) Neutrophil isolation using 1.0875 g/mL Percoll. *Top row:* CD11b⁺CD14^{dim} cells were selected. 3,000 events are displayed in each plot. *Bottom Row:* Neutrophils identified by FSC and SSC. 2,000 events are displayed in each plot. (C) Neutrophil isolation using 1.09 g/mL Percoll. *Top row:* CD11b⁺CD14^{dim} were selected. 3,000 events are displayed in each plot. *Bottom Row:* Neutrophils identified by FSC and SSC. 2,000 events are displayed in each plot.

Optimization of Cell Sorting Procedure for Downstream RNA Isolation and Whole Genome Expression

In order to determine the minimum number of cells that yields sufficient amounts of RNA for gene expression analysis, different quantities of total CD4⁺ T cells and CD8⁺ T cells were sorted by flow cytometry. Samples were prepared, with numbers ranging from 5x10³ to 1x10⁶. In initial samples, unsorted cell samples were maintained on ice until sorted. Sorted cells were collected into RNAprotect and maintained at room temperature. RNA was extracted from each sorted sample and the quantity and quality of extracted RNA was determined. The quality of RNA (intact or degraded) was measured by the RNA integrity number (RIN). RIN values range from 0 to 10, with 10 indicating the highest level of RNA quality⁴⁴. The RINs from all samples were high, ranging from 7.9 to 10 for CD4⁺ T cells and 7.4 to 10 for CD8⁺ T cells. These RIN values indicate highly intact and good quality RNA from our sorted populations. Surprisingly, there was no correlation between cell number and RNA quantity (**Table 2**).

T Cell Type	Cell Number	Total RNA Yield (ng)
CD4	5,000	300.96
CD4	10,000	491.64
CD4	25,000	297.12
CD4	50,000	583.08
CD4	100,000	421.76
CD4	250,000	424.00
CD4	500,000	584.48
CD4	942,500	436.32
CD8	5,000	259.20
CD8	10,000	379.80
CD8	25,000	195.60
CD8	50,000	283.80
CD8	100,000	272.16
CD8	250,000	211.52
CD8	500,000	398.56
CD8	675,500	272.16

Table 2 RNA Yields from Cell Sorting

We repeated the cell sorting and RNA extraction with modifications to the sorting protocol. In the first sort, we had sorted cells into RNAProtect, pelleted the cells by centrifugation, removed supernatant by vacuum aspiration, and resuspended the cells in TRIzol for storage and extraction. We hypothesized that cells were lost during the aspiration step. Therefore in our next sort, we sorted directly into a concentrated form of TRIzol, TRIzol LS, to avoid the pelleting and aspiration steps. This also allowed extraction directly from our sorted cell suspensions. The RNA yields from the cells sorted with this modified procedure showed improved correlation with cell number for samples with at least 2.5×10^5 cells. Likewise, RNA quality was acceptable only in samples with at least 2.5×10^5 cells.

Aim 2. Evaluation of Immune Checkpoint Antibody Panels

PD-L1

Using freshly isolated PBMCs from SIV-naïve monkeys, we performed titrations using a commercially available monoclonal antibody specific for the checkpoint molecule, PD-L1. The molecule was directly conjugated to the fluorochrome phycoerythrin-cyanine 7 (PE-Cy7). Upon analysis, we found substantial non-specific staining of multiple immune cell subsets and determined that this antibody was not appropriate for use in subsequent experiments (data not shown).

Next, we performed multiple titrations to evaluate a different antibody clone specific for PD-L1. This antibody was conjugated to biotin and streptavidin (SA) conjugated to two different fluorochromes were used for detection. Our initial testing was done with SA conjugated to allophycocyanin (APC) but subsequent evaluations were done with SA conjugated to brilliant violet 421 (BV421). We chose to use a biotin-SA staining method because PD-L1 is expressed at extremely low levels on T cells. The biotin-SA method amplifies fluorescent signals compared with a directly conjugated antibody, thus increasing our ability to detect a positive signal. In addition, SA has high affinity and specificity for biotin and therefore should not contribute to background fluorescence⁴⁵.

Using cryopreserved PBMCs from two SIV-naïve monkeys, we tested the PD-L1-biotin antibody. One-half of the cells were stimulated overnight with phorbol 12-myristate 13-acetate (PMA) and ionomycin and the other half were left unstimulated. Five concentrations of PD-L1-biotin were evaluated: 1.25, 2.5, 5, 10, and 20 µg/mL. The

concentration of SA- APC was kept constant at 1 $\mu\text{g}/\text{mL}$. We analyzed B cells, NK cells, T cells, and monocytes. All concentrations that were tested showed similar staining. A representative plot is given in **Figure 4**.

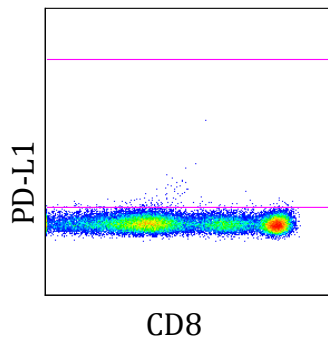


Figure 4 PD-L1 staining of T cells stimulated with PMA/Ionomycin

Representative flow plot shows PD-L1 staining on stimulated T cell. The biotin-labeled anti-PD-L1 antibody was titrated between 1.25 and 20 $\mu\text{g}/\text{mL}$. All concentrations showed similar staining to that of the lowest concentration (1.25 $\mu\text{g}/\text{mL}$).

Because there was similar staining at all concentrations of the PD-L1 antibody, we retitrated it at lower concentrations. We chose to test concentrations of 0.75, 1.5, and 2.5 $\mu\text{g}/\text{mL}$. The concentration of SA-BV421 was kept constant at 1 $\mu\text{g}/\text{mL}$. Cells from two SIV-naïve monkeys were split, with one-half being stimulated with PMA and ionomycin overnight and the other half being left unstimulated. Upon analysis, we noted substantial background staining for B cells as well as T cells, even at the lowest concentration for both stimulated and unstimulated cells. Representative flow plots for both B and T cells are shown in **Figure 5A**.

The persistence of high background staining led us to test one additional set of PD-L1 antibody concentrations: 0.1, 0.25, 0.75, and 1.5 $\mu\text{g}/\text{mL}$. The concentration of SA-

BV421 was kept constant at a lower value of 0.25 $\mu\text{g}/\text{mL}$. Staining was performed with cryopreserved PBMCs from one chronically infected monkey and one naïve monkey.

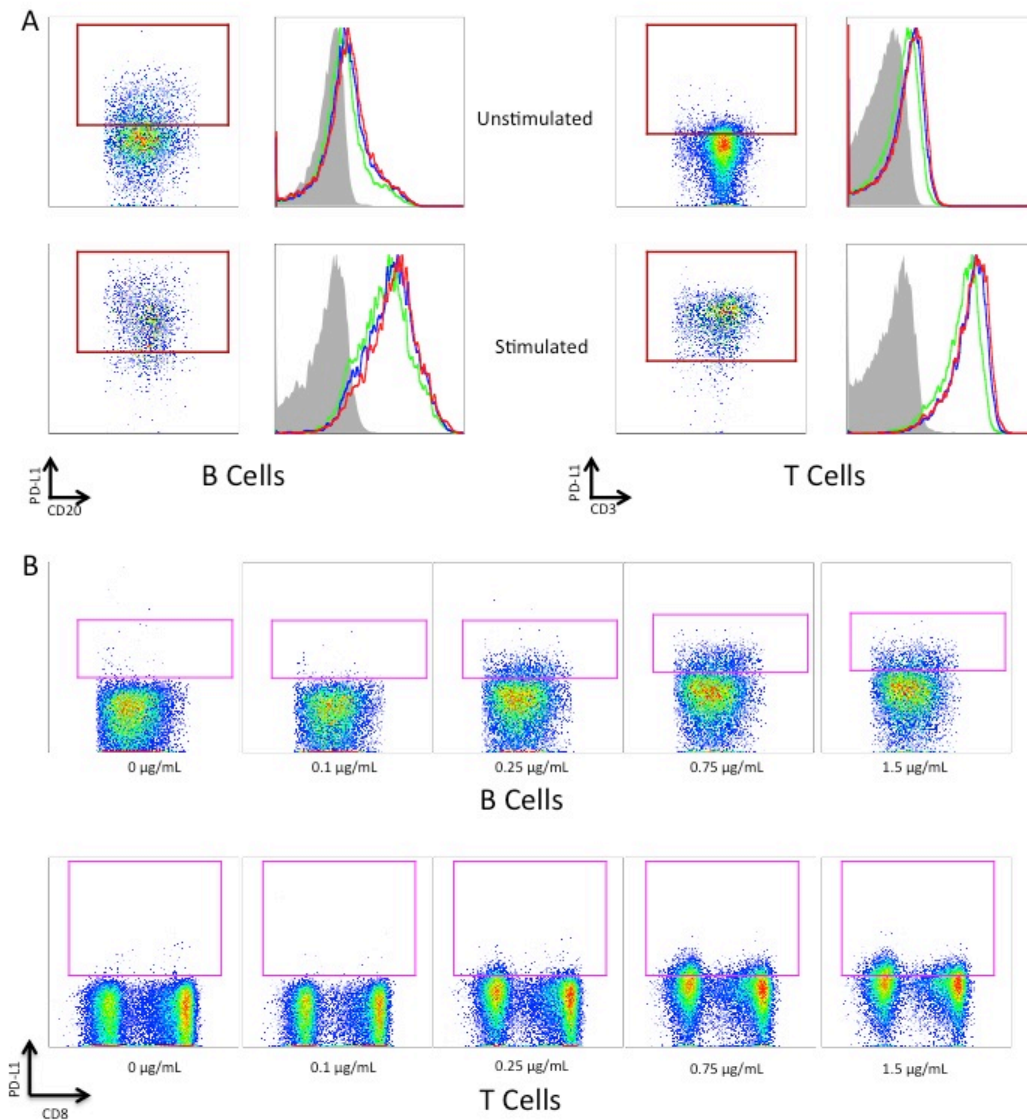


Figure 5 PD-L1 Titrations (A) Representative flow plots for staining of B (left) and T (right) cells with PD-L1-biotin-SA-BV421. Shaded gray histograms represent background fluorescence in the absence of antibody. Green: 0.75 $\mu\text{g}/\text{mL}$, blue: 1.5 $\mu\text{g}/\text{mL}$, red: 2.5 $\mu\text{g}/\text{mL}$. (B) Ex vivo PD-L1 staining at 0, 0.1, 0.25, 0.75, and 1.5 $\mu\text{g}/\text{mL}$. *Top row:* B cells. *Bottom row:* T cells.

There was no positive staining using 0.1 $\mu\text{g}/\text{mL}$ of antibody. Modest background staining was observed using 0.25 $\mu\text{g}/\text{mL}$. While the level of background staining was higher, particularly on T cells using 0.75 $\mu\text{g}/\text{mL}$, this higher concentration appeared necessary to detect PD-L1⁺ B cells (**Figure 5B**). Therefore, the final antibody concentration chosen for PD-L1 was 0.75 $\mu\text{g}/\text{mL}$.

Finally, we performed titrations of SA-BV421. We tested SA-BV421 at concentrations of 0.5, 1, and 2 $\mu\text{g}/\text{mL}$. The antibody against PD-L1 was kept constant at 2.5 $\mu\text{g}/\text{mL}$. Cells were stimulated with PMA and ionomycin overnight. Staining of was similarly strong among all concentrations (data not shown). We then tested SA-BV421 at concentrations of 0.25, 0.5, and 1 $\mu\text{g}/\text{mL}$ while the concentration of the anti-PD-L1 was kept constant at 2.5 $\mu\text{g}/\text{mL}$. Staining was similarly strong among all concentrations tested (data not shown). Therefore, the final antibody concentration for SA-BV421 chosen was 0.25 $\mu\text{g}/\text{mL}$.

LAG-3

We performed multiple titrations of a monoclonal antibody specific for another checkpoint molecule of interest, LAG-3, conjugated to the fluorochrome phycoerythrin (PE). Cryopreserved PBMCs from two SIV-naïve monkeys were thawed and split, with one half being stimulated with concanavalin (ConA) or left unstimulated. We evaluated the anti-LAG-3 antibody at concentrations of 2.5, 5, 10, 20, 40, and 100 $\mu\text{g}/\text{mL}$. T cells were analyzed and positive populations were detected even at the lowest concentration (2.5 $\mu\text{g}/\text{mL}$) for both stimulated and unstimulated cells (**Figure 6A**). At higher

concentrations, the amount of background staining increased substantially (data not shown).

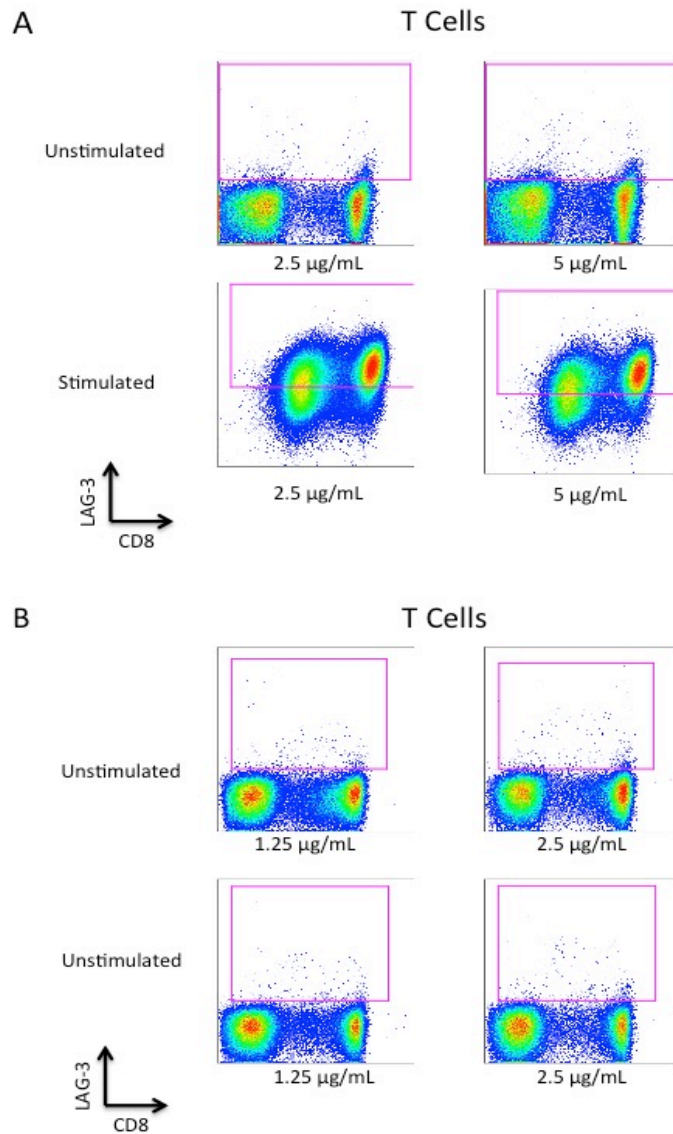


Figure 6 LAG-3 titration

(A) Flow plots show staining of T cells with anti-LAG-3 in both unstimulated and stimulated samples at 2.5 and 5 µg/mL. (B) Flow plots show staining of T cells with anti-LAG-3 antibody in unstimulated samples and 1.25 and 2.5 µg/mL.

Because positive staining was observed at the lowest concentration tested (2.5 $\mu\text{g}/\text{mL}$), the anti-LAG-3 antibody was titrated at lower concentrations (0.3, 0.6, 1.25, and 2.5 $\mu\text{g}/\text{mL}$) on unstimulated cells from two additional monkeys. Separation of LAG-3⁺ cells was best seen at 2.5 $\mu\text{g}/\text{mL}$ (**Figure 6B**) and we chose this value as our final antibody concentration.

TIM-3

We performed multiple titrations of a monoclonal antibody specific for another checkpoint molecule of interest, TIM-3. *Ex vivo* staining was performed on PBMCs from two chronically SIV infected monkeys. The TIM-3 antibody conjugated to the fluorochrome AlexaFluor488 (A488) was tested at concentrations of 2.5, 5, 10, and 20 $\mu\text{g}/\text{mL}$. We were most interested in expression of TIM-3 in T cells. Upon analysis, there was increased background staining of T cells at and above 10 $\mu\text{g}/\text{mL}$ (**Figure 7A**).

Background staining of T cells at 2.5 $\mu\text{g}/\text{mL}$ and 5 $\mu\text{g}/\text{mL}$ was similar to that without antibody, while higher concentrations of 10 $\mu\text{g}/\text{mL}$ and 20 $\mu\text{g}/\text{mL}$ gave significantly increased background staining. Unexpectedly, we also observed positive staining of a subset of B cells (**Figure 7B**). These concentrations were again tested but on PBMCs after stimulation with ConA for 3 days.

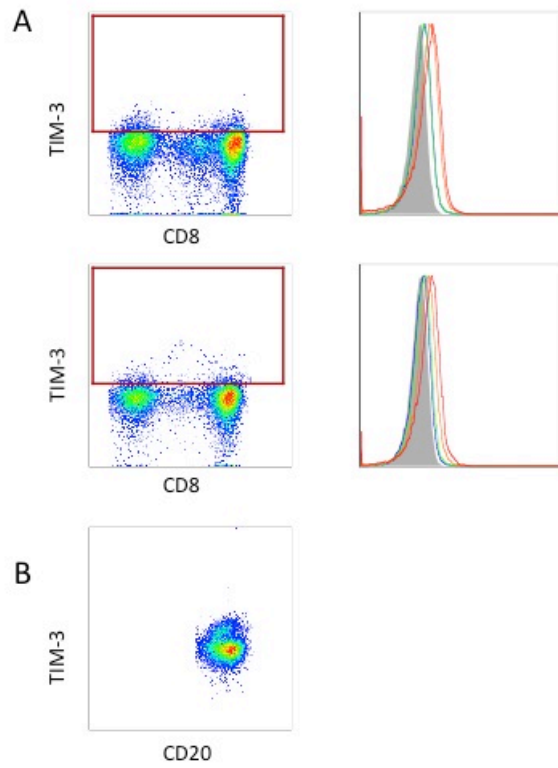


Figure 7 TIM-3-A488 staining

(A) Flow plots show TIM-3 staining on T cells at 10 $\mu\text{g/mL}$. Staining at concentrations greater than 10 $\mu\text{g/mL}$ was similar. Histograms show staining of all concentrations evaluated. The shaded area represents background fluorescence in the absence of antibody. Blue: 2.5 $\mu\text{g/mL}$, green: 5 $\mu\text{g/mL}$, orange: 10 $\mu\text{g/mL}$, red: 20 $\mu\text{g/mL}$. (B) Flow plot shows TIM-3 staining on B cells.

Staining was compared with the same antibody conjugated to the fluorochrome APC, which had been titrated previously. T cells were analyzed for TIM-3 expression. Both 2.5 and 5 $\mu\text{g/mL}$ of the A488 conjugate showed similar staining to the APC conjugate at 10 $\mu\text{g/mL}$ (**Figure 8**)

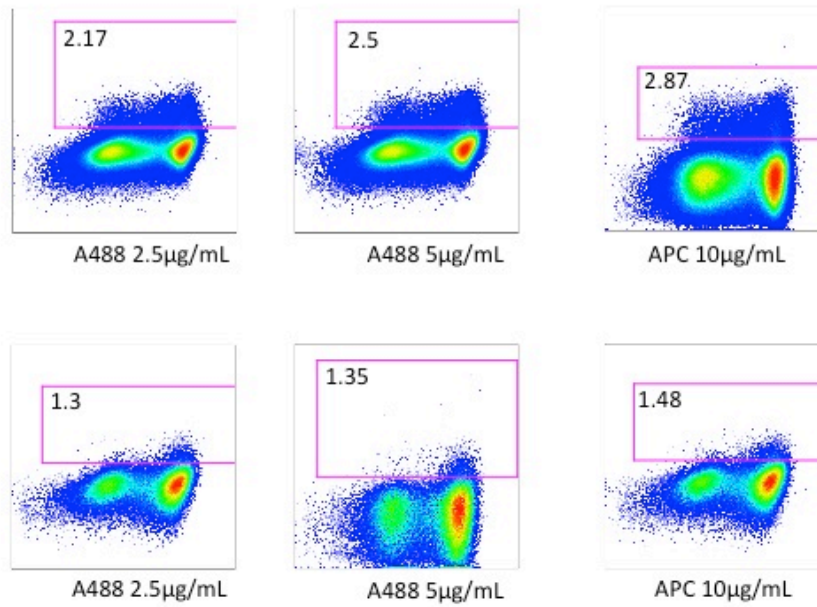


Figure 8 Detection of TIM-3⁺ T cells with A488 and APC conjugates

Staining of T cells by the anti-TIM-3 antibody. T cells were stained with the A488 conjugate are compared to those stained with the APC conjugate.

DISCUSSION

Aim 1. Isolation of Cells and RNA for Gene Expression Deconvolution

A majority of immune cell subsets are modified during HIV infection. There is considerable interest in understanding the nature of these changes to help facilitate the development of HIV immunotherapies. Whole genome expression analysis facilitates a detailed understanding of biological perturbations on a cellular level. A recent bioinformatics method, expression deconvolution, utilizes existing gene expression data to measure changes of discrete cell subpopulations within a heterogeneous cell sample. While the tools for this method have been developed for human samples, they do not exist for rhesus monkey samples. Therefore, we took the first steps in the process of developing these bio-informatic tools for rhesus monkeys. This process required developing methods to detect rhesus immune cell subsets from peripheral blood and isolate their RNA. Major peripheral blood immune cell subsets were chosen to target for identification and cell sorting. Definitions of target subsets were based on expression of particular cell surface proteins and were further divided based on activation status. Our technical assessment of the antibody panels demonstrated that there were no adverse interactions between fluorochromes in any of the antibody panels.

Initially, activated T cells were defined based on positive expression of two proteins, HLA-DR and CD38. However, our initial assessment of these proteins as markers to identify activated cells found that the frequency of the activated cells was remarkably low. This was not the case with our other target cell subsets, which were readily identified. To address this issue, we chose to use the expression of the cell surface

protein, CD69, as the definition of activated T cells. A revised panel using CD69 as an activation marker for T cells was tested and analyzed. The frequency of CD69⁺ T cells was substantially higher than CD38-positive, HLA-DR-positive T cells as defined in the original staining panel. Again, no adverse interactions were noted between fluorochromes in this revised panel.

While neutrophils have not been a cell subset of primary focus in HIV research, they account for up to 60% of all nucleated cells in the peripheral blood⁴⁶. Therefore, in developing a method for parsing of gene expression signals that belong to different cell subsets, it is crucial to identify of and adjust the signal from neutrophils is crucial. We initially attempted to sort neutrophils based on their light scattering properties; however, this could not be accomplished reliably. As a result, we chose to develop a separate neutrophil isolation procedure. Our evaluation of multiple commercially available products designed for human blood was unsuccessful. Although, the cellular composition and density of cells are similar between humans and rhesus monkeys, there are differences that have been previously identified that are substantial enough such that products designed for human samples are not compatible with rhesus monkey samples. In using density gradient centrifugation for cell subset isolation, the specific cell density determines the layer into which the cell populations will segregate. Differences in neutrophil density between humans and rhesus monkeys may explain the inability to isolate rhesus neutrophils using products designed for human blood.

This issue led us to assess Percoll concentrations that were slightly less dense than the products used for human samples. In doing so, we found that Percoll of density 1.09

g/mL was optimal for both yield and purity of rhesus neutrophils (with concomitant isolation of PBMCs with a Percoll layer of density 1.077 g/mL). This is similar to a previous report in 1991⁴⁷ that demonstrated Ficoll of 1.077 g/mL combined with Ficoll of 1.100 g/mL was optimal for simultaneous isolation of PBMCs and neutrophils, respectively, from rhesus peripheral blood.

Overall, we successfully developed three antibody panels and a separate Percoll-based method. When combined, these methods allow for detection and sorting of the following immune cell subsets, which account for essentially all nucleated cells in whole blood of rhesus monkeys. These immune cell subsets are as follows: monocytes, pDCs, mDCs, neutrophils, activated and resting CD4⁺ T cells, activated and resting CD8⁺ T cells, activated and resting B cells, and activated and resting NK cells.

To determine the minimum number of cells necessary to yield sufficient amounts of RNA for gene expression analysis, we sorted different numbers of total CD4⁺ T cells and CD8⁺ T cells by flow cytometry. RNA obtained from these cells was subsequently analyzed for quality using RIN. RIN values range from 0 to 10, with 10 indicating the highest quality RNA. While the quality of RNA obtained from these sorts was high, there was no correlation between cell number and total RNA yield. This result suggested that either the cells or the RNA was being lost during one of the steps in the protocol.

Consequently, we repeated our cell sorting and RNA extraction but with minor modifications to the protocol. Initially, cells were sorted into RNAProtect and pelleted by centrifugation, supernatant was aspirated, and the cells were resuspended in TRIzol. Loss of cells during the aspiration step appeared to be the cause of the inconsistency between

cell number and RNA yield. In the revised protocol, we sorted cells directly into a concentrated form of TrRIzol, TRIzol LS, which allowed for direct extraction. The total RNA extracted exhibited improved correlation with cell number but only with populations with at least 2.5×10^5 cells. RIN was also only acceptable at these higher populations. Therefore, we successfully optimized a procedure to sort and extract RNA of a quality and quantity that was sufficient for downstream whole genome expression analysis.

One potential limitation to this approach is that several of the immune cell subsets are extremely rare *in vivo*. For example, pDCs account for only 0.2% of all white blood cells in peripheral blood^{48,49}. Even from large samples of whole blood, we may not obtain the number (2×10^5 cells) that was determined to be the minimum amount for reliable RNA isolation. One alternative approach would be to culture and expand cells *in vitro*. Unfortunately, these cultured cells would need to be modified to allow for expansion, which would be contradictory to our goal of providing physiological gene expression data in a naïve population. Alternatively, methods have recently been developed that allow for whole genome sequencing from a small number of cells, down to single cells⁵⁰. This method could be used to generate whole genome expression data from those cell subsets for which the cell numbers sorted *ex vivo* are insufficient for standard whole genome expression methods requiring large cell numbers.

Aim 2. Evaluation of Immune Checkpoint Antibody Panels

HIV infection leads to various detrimental effects on immunity. It creates a state of sustained immune hyperactivation^{21,51} that leads to end organ damage and disease¹⁶ even with control of viremia. Sustained hyperimmune activation also promotes increased expression of negative regulatory molecules (checkpoint molecules) such as LAG-3, TIM-3, and PD-1 as well as its ligands, PD-L1 and PD-L2. HIV preferentially infects CD4⁺ T cells and induces their rapid decline. While there is a compensatory expansion of virus-specific CD8⁺ T cells, these cells exhibit broad functional defects related to survival, proliferation, cytokine production, and cytotoxic ability⁵². These defects are associated with expression of checkpoint molecules. For example, LAG-3 exhibits considerable homology to CD4 and binds MHC II on APCs to limit T cell activation⁵³. Expression of PD-1 is also correlated to plasma viremia²⁰. There is also expansion of regulatory T cells that express a variety of these checkpoint molecules including TIM-3 and cytotoxic T-lymphocyte associated protein 4 (CTLA-4)^{54,55}.

Binding of these checkpoint molecules with their ligands not only dampens immune responses, an action which is necessary to limit immune-mediated tissue damage, but also perpetuates the negative effects of HIV infection. Many researchers in the field are investigating these molecules to better characterize and understand their expression on different immune cell types in hope of targeting them for HIV treatment. In fact, antibodies directed against these checkpoint molecules have been used in the treatment of different cancers. Anti-PD-1 has been applied to in the treatment of hematologic cancers with moderate success³⁷ and anti-CTLA-4, when combined with

current therapies has resulted in improved responses to treatment in metastatic melanoma patients⁵⁴. The immune defects observed in cancer are similar to those observed in chronic HIV infection. To develop tools to study these molecules in SIV-infected rhesus monkeys, we set out to optimize the use of antibodies specific to PD-L1, LAG-3, and TIM-3 for use in flow cytometric analysis.

To detect cells expressing PD-L1, we ultimately chose to use a biotinylated anti-PD-L1 antibody along with a fluorescently conjugated SA for multiple reasons. It is well documented that binding and specificity between biotin and SA are very high⁴⁵. Additionally, the biotin-SA antibody method increases the fluorescent signal, facilitating more sensitive detection of positive cells. Finally, the directly conjugated PD-L1 that we evaluated showed substantial non-specific staining of immune cells and was unsuitable for future experiments.

Initially, we tested PD-L1-biotin on both stimulated and unstimulated PBMCs. PD-L1 is expressed on a subset of B cells and monocytes *ex vivo* without stimulation and is substantially upregulated on these cells upon stimulation. PD-L1 is generally not expressed on resting T cells; stimulation is required. Therefore, comparison of stimulated and un-stimulated samples was used to assess whether the antibody was binding specifically to PD-L1. In stimulated samples, we observed that a substantial percentage of all immune subsets exhibited positive staining compared to un-stimulated samples. This observation suggested that the antibody was binding to the expected target.

The range of antibody concentrations used in the first two evaluations showed substantial fluorescent signal, even with unstimulated T cells, which should be negative.

This situation implied that we were using excessive amounts of antibody leading to non-specific staining. To address this issue, we tested lower concentrations of antibody along with a lower concentration of SA-BV421. Staining with 0.25 $\mu\text{g}/\text{mL}$ of SA-BV421 resulted in minimal background staining; however, it prevented detection of all PD-L1-positive cells. Conversely, staining with 0.75 $\mu\text{g}/\text{mL}$ showed modest increases in background staining, but allowed for enhanced detection of PD-L1-positive cells. Therefore, the 0.75 $\mu\text{g}/\text{mL}$ concentration may be used for future experiments, although we must be cautious about misinterpreting low levels of background for true PD-L1-positive cells. Alternatively, we may consider evaluating a different antibody clone.

For the detection of cells expressing LAG-3, we stained both stimulated and unstimulated cryopreserved PBMCs. LAG-3 has been reported to be expressed on B cells, and NK cells, and activated T cells⁵³. We were most interested in the expression of LAG-3 on T cells because of its negative regulatory effects on proliferation and activation, which are thought to dampen the immune response against HIV⁵⁶. During our first titration, all concentrations (2.5-100 $\mu\text{g}/\text{mL}$) tested exhibited positive staining of T cells. There were substantially higher percentages found in the stimulated samples compared with the unstimulated samples, demonstrating the specificity of detection. However, the background fluorescence was extremely high at 10 $\mu\text{g}/\text{mL}$ and it was not clear that even the lowest concentration evaluated (2.5 $\mu\text{g}/\text{mL}$) was the optimal concentration. As a result, we repeated the experiment but with lower concentrations of antibody with *ex vivo* PBMCs. Although we saw positive staining at both 1.25 $\mu\text{g}/\text{mL}$ and 2.5 $\mu\text{g}/\text{mL}$, the best detection and separation of LAG-3-positive T cells was at 2.5 $\mu\text{g}/\text{mL}$.

Our final evaluation was of an antibody to detect TIM-3. TIM-3 is expressed on T cells, DCs, and monocytes⁵³. We were most interested in TIM-3 expression on T cells because of its negative proliferative effects and pro-apoptotic effect on T helper (T_H) cells⁵⁵. Our first evaluation of the antibody on un-stimulated cells was not informative, since very few T cells express TIM-3 without stimulation. Upon staining of stimulated cells, we found that the 2.5 µg/mL concentration gave optimal staining and therefore could be used for future experiments.

Expression of TIM-3 has not been reported in B cells. Thus, we were surprised to find apparent specific staining of a subpopulation of B cells with this TIM-3 antibody. It is possible that this antibody was detecting another protein in addition to its target protein, TIM-3. If this is the case, it may be necessary to evaluate an additional TIM-3 antibody clone. Otherwise, the expression of TIM-3 on B cells in these rhesus monkey samples may be real, revealing a difference in tissue expression between humans and rhesus monkeys. While humans and monkeys share substantial physiology and molecular biology, there are a number of subtle differences in protein homology and tissue expression that have been reported. For examples, NK cells in humans do not express the CD8 molecule, whereas NK cells in rhesus monkeys do. Therefore, we may have uncovered such a difference in protein expression. This variation should be explored further because knowledge these differences can inform the translation of findings between rhesus monkeys and humans.

Future Directions

We have optimized the detection of three proteins that play a central role in the defective immune responses against HIV and therefore whose understanding of is vital to develop immunotherapies. The fluorochromes conjugated to antibodies targeting these proteins were carefully selected in order to allow for optimal protein detection while minimizing adverse interactions between them. The next step will be to combine these antibodies, as well as additional antibodies, into a comprehensive antibody panel. Because some of these additional antibodies will be limited in their fluorochrome availability, we had to keep this in mind when selecting the fluorochromes that PD-L1, LAG-3, and TIM-3 antibodies were conjugated to. This comprehensive antibody panel will not only be able to detect these three proteins simultaneously, but will also be able to detect multiple other proteins known to be important for assessing T cell phenotype and T cell activation. Therefore, this antibody panel will be critical in detecting, quantifying, and tracking the expression of these molecules on immune cell subsets in SIV-infected rhesus monkeys, and the results will be vital in developing effective immunotherapies against HIV.

LIST OF JOURNAL ABBREVIATIONS

ANNU REV BIOCHEM annual review of biochemistry

ANNU REV IMMUNOL annual review of immunology

APPL MICROBIOL BIOTECHNOL applied microbiology and biotechnology

BLOOD REV blood reviews

BMC INFECT DIS bmc infectious diseases

BMC MOL BIOL bmc molecular biology

BR MED J CLIN RES ED british medical journal clinical research edition

CELL IMMUNOL cellular immunology

COLD SPRING HARB PERSPECT MED cold spring harbor perspectives in medicine

CURR OPIN HIV AIDS current opinions in hiv and aids

CURR OPIN MICROBIOL current opinion in microbiology

CURR OPIN VIROL current opinion in virology

GENES IMMUN genes and immunity

HOPKINS HIV REP BIMON NEWSL HEALTHC PROVIDE JOHNS HOPKINS

UNIV AIDS SERV the hopkins hiv report: a bimonthly newsletter for healthcare providers / johns hopkins university aids service

IMMUNOL LETT immunology letters

IMMUNOL REV immunology reviews

J CLIN ONCOL journal of clinical oncology

J EXP MED journal of experimental medicine

J IMMUNOL journal of immunology

J MED PRIMATOL journal of medical primatology

J VIROL journal of virology

J VIS EXP journal of visualized experiments

MOL IMMUNOL molecular immunology

NAT GENET nature genetics

NAT MED nature medicine

N ENGL J MED new england journal of medicine

NUCLEIC ACIDS RES nucleic acids research

REV MED VIROL reviews in medical virology

SCI TRANSL MED science translational Medicine

REFERENCES

1. WHO | Data and statistics. *WHO* at <<http://www.who.int/hiv/data/en/>>
2. Gottlieb, M. S. *et al.* *Pneumocystis carinii* Pneumonia and Mucosal Candidiasis in Previously Healthy Homosexual Men: Evidence of a New Acquired Cellular Immunodeficiency. *N. Engl. J. Med.* **305**, 1425–1431 (1981).
3. Gerstoft, J. *et al.* Severe acquired immunodeficiency in European homosexual men. *Br. Med. J. Clin. Res. Ed* **285**, 17–19 (1982).
4. Barré-Sinoussi, F. *et al.* Isolation of a T-lymphotropic retrovirus from a patient at risk for acquired immune deficiency syndrome (AIDS). *Science* **220**, 868–871 (1983).
5. Frankel, A. D. & Young, J. A. HIV-1: fifteen proteins and an RNA. *Annu. Rev. Biochem.* **67**, 1–25 (1998).
6. Biebricher, C. K. & Eigen, M. What is a quasispecies? *Curr. Top. Microbiol. Immunol.* **299**, 1–31 (2006).
7. Kwong, P. D. *et al.* Structure of an HIV gp120 envelope glycoprotein in complex with the CD4 receptor and a neutralizing human antibody. *Nature* **393**, 648–659 (1998).
8. Berson, J. F. *et al.* A seven-transmembrane domain receptor involved in fusion and entry of T-cell-tropic human immunodeficiency virus type 1 strains. *J. Virol.* **70**, 6288–6295 (1996).

9. Feng, Y., Broder, C. C., Kennedy, P. E. & Berger, E. A. HIV-1 entry cofactor: functional cDNA cloning of a seven-transmembrane, G protein-coupled receptor. *Science* **272**, 872–877 (1996).
10. Zhou, Y., Zhang, H., Siliciano, J. D. & Siliciano, R. F. Kinetics of Human Immunodeficiency Virus Type 1 Decay following Entry into Resting CD4+ T Cells. *J. Virol.* **79**, 2199–2210 (2005).
11. Nyamweya, S. *et al.* Comparing HIV-1 and HIV-2 infection: Lessons for viral immunopathogenesis. *Rev. Med. Virol.* **23**, 221–240 (2013).
12. Sharp, P. M. & Hahn, B. H. Origins of HIV and the AIDS Pandemic. *Cold Spring Harb. Perspect. Med.* **1**, a006841–a006841 (2011).
13. McDougal, J. S. *et al.* Binding of HTLV-III/LAV to T4+ T cells by a complex of the 110K viral protein and the T4 molecule. *Science* **231**, 382–385 (1986).
14. Larsson, M. *et al.* Molecular signatures of T-cell inhibition in HIV-1 infection. *Retrovirology* **10**, 31 (2013).
15. Spano, J.-P. *et al.* AIDS-Related Malignancies: State of the Art and Therapeutic Challenges. *J. Clin. Oncol.* **26**, 4834–4842 (2008).
16. Deeks, S. G., Tracy, R. & Douek, D. C. Systemic Effects of Inflammation on Health during Chronic HIV Infection. *Immunity* **39**, 633–645 (2013).
17. Murray, J. M. *et al.* HIV DNA Subspecies Persist in both Activated and Resting Memory CD4+ T Cells during Antiretroviral Therapy. *J. Virol.* **88**, 3516–3526 (2014).

18. Barouch, D. H. & Deeks, S. G. Immunologic strategies for HIV-1 remission and eradication. *Science* **345**, 169–174 (2014).
19. Chomont, N. *et al.* HIV reservoir size and persistence are driven by T cell survival and homeostatic proliferation. *Nat. Med.* **15**, 893–900 (2009).
20. Klatt, N. R., Chomont, N., Douek, D. C. & Deeks, S. G. Immune activation and HIV persistence: implications for curative approaches to HIV infection. *Immunol. Rev.* **254**, 326–342 (2013).
21. Wilson, E. B. *et al.* Blockade of Chronic Type I Interferon Signaling to Control Persistent LCMV Infection. *Science* **340**, 202–207 (2013).
22. Lahaye, X. & Manel, N. Viral and cellular mechanisms of the innate immune sensing of HIV. *Curr. Opin. Virol.* **11C**, 55–62 (2015).
23. Heil, F. *et al.* Species-specific recognition of single-stranded RNA via toll-like receptor 7 and 8. *Science* **303**, 1526–1529 (2004).
24. Biron, C. A. Initial and innate responses to viral infections--pattern setting in immunity or disease. *Curr. Opin. Microbiol.* **2**, 374–381 (1999).
25. Lee, S. H. *et al.* Susceptibility to mouse cytomegalovirus is associated with deletion of an activating natural killer cell receptor of the C-type lectin superfamily. *Nat. Genet.* **28**, 42–45 (2001).
26. Alter, G. *et al.* HLA Class I Subtype-Dependent Expansion of KIR3DS1+ and KIR3DL1+ NK Cells during Acute Human Immunodeficiency Virus Type 1 Infection. *J. Virol.* **83**, 6798–6805 (2009).

27. Bartlett, J. G. The DHHS adult ART guidelines are revised. *Hopkins HIV Rep. Bimon. Newsl. Healthc. Provid. Johns Hopkins Univ. AIDS Serv.* **17**, 6–7 (2005).
28. Luque, M. C. *et al.* Gene expression profile in long-term non progressor HIV infected patients: In search of potential resistance factors. *Mol. Immunol.* **62**, 63–70 (2014).
29. Meijerink, H. *et al.* The number of CCR5 expressing CD4+ T lymphocytes is lower in HIV-infected long-term non-progressors with viral control compared to normal progressors: a cross-sectional study. *BMC Infect. Dis.* **14**, (2014).
30. Hatzioannou, T. & Evans, D. T. Animal models for HIV/AIDS research. *Nat. Rev. Microbiol.* **10**, 852–867 (2012).
31. Brenchley, J. M. *et al.* Differential infection patterns of CD4+ T cells and lymphoid tissue viral burden distinguish progressive and nonprogressive lentiviral infections. *Blood* **120**, 4172–4181 (2012).
32. Paiardini, M. *et al.* Low levels of SIV infection in sooty mangabey central memory CD4+ T cells are associated with limited CCR5 expression. *Nat. Med.* **17**, 830–836 (2011).
33. Li, Q. *et al.* Peak SIV replication in resting memory CD4+ T cells depletes gut lamina propria CD4+ T cells. *Nature* (2005). doi:10.1038/nature03513
34. Evans, D. T. & Silvestri, G. Nonhuman primate models in AIDS research. *Curr. Opin. HIV AIDS* **8**, 255–261 (2013).
35. Brenchley, J. M. & Douek, D. C. Microbial translocation across the GI tract. *Annu. Rev. Immunol.* **30**, 149–173 (2012).

36. George, M. D. *et al.* Transcriptional profiling of peripheral CD8+T cell responses to SIV Δ nef and SIVmac251 challenge reveals a link between protective immunity and induction of systemic immunoregulatory mechanisms. *Virology* **468-470**, 581–591 (2014).
37. Bryan, L. J. & Gordon, L. I. Blocking tumor escape in hematologic malignancies: The anti-PD-1 strategy. *Blood Rev.* (2014). doi:10.1016/j.blre.2014.09.004
38. Abbas, A. R. *et al.* Immune response in silico (IRIS): immune-specific genes identified from a compendium of microarray expression data. *Genes Immun.* **6**, 319–331 (2005).
39. Gong, T. *et al.* Optimal Deconvolution of Transcriptional Profiling Data Using Quadratic Programming with Application to Complex Clinical Blood Samples. *PLoS ONE* **6**, e27156 (2011).
40. Funaro, A. *et al.* Involvement of the multilineage CD38 molecule in a unique pathway of cell activation and proliferation. *J. Immunol.* **145**, 2390–2396 (1990).
41. Palacios, R. & Möller, G. HLA-DR antigens render resting T cells sensitive to Interleukin-2 and induce production of the growth factor in the autologous mixed lymphocyte reaction. *Cell. Immunol.* **63**, 143–153 (1981).
42. Lopez-Cabrera, M. Molecular cloning, expression, and chromosomal localization of the human earliest lymphocyte activation antigen AIM/CD69, a new member of the C-type animal lectin superfamily of signal-transmitting receptors. *J. Exp. Med.* **178**, 537–547 (1993).

43. Oh, H., Siano, B. & Diamond, S. Neutrophil isolation protocol. *J. Vis. Exp.* (2008).
doi:10.3791/745
44. Schroeder, A. *et al.* The RIN: an RNA integrity number for assigning integrity values to RNA measurements. *BMC Mol. Biol.* **7**, 3 (2006).
45. Dundas, C. M., Demonte, D. & Park, S. Streptavidin-biotin technology: improvements and innovations in chemical and biological applications. *Appl. Microbiol. Biotechnol.* **97**, 9343–9353 (2013).
46. Blood differential: MedlinePlus Medical Encyclopedia. at
<<http://www.nlm.nih.gov/medlineplus/ency/article/003657.htm>>
47. Taniuchi, S. Isolation of functional polymorphonuclear leukocytes from rhesus monkeys using discontinuous Ficoll-Hypaque density gradients. *J. Med. Primatol.* **20**, 271–274 (1991).
48. Baumgart, D. C. *et al.* Patients with active inflammatory bowel disease lack immature peripheral blood plasmacytoid and myeloid dendritic cells. *Gut* **54**, 228–236 (2005).
49. MacDonald, K. P. A. *et al.* Characterization of human blood dendritic cell subsets. *Blood* **100**, 4512–4520 (2002).
50. Saliba, A.-E., Westermann, A. J., Gorski, S. A. & Vogel, J. Single-cell RNA-seq: advances and future challenges. *Nucleic Acids Res.* **42**, 8845–8860 (2014).
51. Teijaro, J. R. *et al.* Persistent LCMV Infection Is Controlled by Blockade of Type I Interferon Signaling. *Science* **340**, 207–211 (2013).

52. Favre, D. *et al.* HIV disease progression correlates with the generation of dysfunctional naive CD8^{low} T cells. *Blood* **117**, 2189–2199 (2011).
53. Shih, K., Arkenau, H.-T. & Infante, J. R. Clinical Impact of Checkpoint Inhibitors as Novel Cancer Therapies. *Drugs* **74**, 1993–2013 (2014).
54. Kvistborg, P. *et al.* Anti-CTLA-4 therapy broadens the melanoma-reactive CD8⁺ T cell response. *Sci. Transl. Med.* **6**, 254ra128–254ra128 (2014).
55. Moorman, J. P. *et al.* Tim-3 Pathway Controls Regulatory and Effector T Cell Balance during Hepatitis C Virus Infection. *J. Immunol.* **189**, 755–766 (2012).
56. Li, F.-J., Zhang, Y., Jin, G.-X., Yao, L. & Wu, D.-Q. Expression of LAG-3 is coincident with the impaired effector function of HBV-specific CD8⁺ T cell in HCC patients. *Immunol. Lett.* **150**, 116–122 (2013).

CURRICULUM VITAE
Jessica Nguyen
Nguyen.jessica.h@gmail.com
1989

EDUCATION

Boston University, Boston, MA
Master of Science, Medical Sciences
Cumulative GPA: 3.86
Expected May 2015

University of California Santa Barbara, Santa Barbara, CA
Bachelor of Science, Biological Sciences
Cumulative GPA: 3.45
June 2011

University of Edinburgh, Edinburgh, Scotland, UK
Fall semester study abroad immersion program
September-December 2009

PROFESSIONAL EXPERIENCE

Center for Virology and Vaccine Research, Beth Israel Deaconess Medical Center, Boston, MA 08/2014-Present

Research Graduate Student

1. Assisting with weekly blood processing
2. Knowledge and experience with flow cytometry and antibody staining

Medical Scribe Systems, El Segundo, CA 08/2011-08/2013

Travel Trainer

1. Traveled on 6 week long projects across the country training newly hired emergency department scribes
2. Extensive training and practical experience with electronic medical record systems including Epic, Cerner, and Meditech
3. Worked as liaison between corporate offices in California and physician group directors on site

VOLUNTEER EXPERIENCE

Squashbusters, Inc., Boston, MA 01/2014-Present

Academic Coach

Adventures in Caring, Santa Barbara, CA 11/2007-04/2011

Volunteer at Alexander Gardens Assisted Living